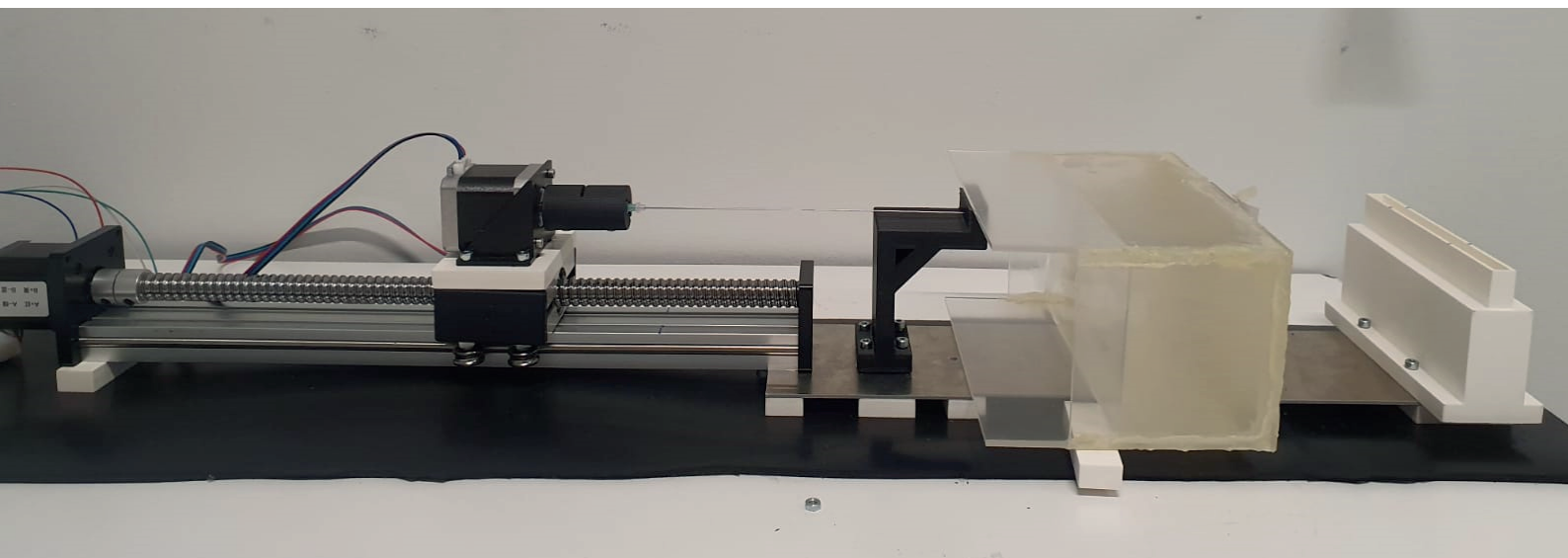


The influence of rotation on the precision of needle end-point position in lateral direction for biopsy

MSc thesis Mechanical Engineering



THE INFLUENCE OF ROTATION ON THE PRECISION OF NEEDLE
END-POINT POSITION IN LATERAL DIRECTION FOR BIOPSY

A master thesis submitted to the Delft University of Technology in partial fulfillment
of the requirements for the degree of

Master of Science in Mechanical Engineering

by
L. P. N. Koopman
August 2021

The work in this thesis was made in the:

Department of BioMechanical Engineering
Faculty of Mechanical, Maritime & Material
Engineering
Delft University of Technology

Thesis committee: Dr. J. J. van den Dobbelsteen
Dr. ir. M. C. Plooij
Ir. M. de Vries

ABSTRACT

Breast cancer is currently the most prevalent type of cancer. The concluding diagnosis can be obtained with an MRI-guided biopsy. However, due to respiratory movement and human error, the procedure can require multiple attempts, resulting in harmful consequences. To reach the target at the first attempt, the precision of the procedure should be increased, and a robotic system can aid in this. An MRI-compatible concept is designed, but two of its working principles need to be researched before further development.

A possible solution for increasing precision is rotating the needle along the insertion axis. Literature has studied the effect rotation has on insertion force, tissue indentation and target displacement in axial direction, which all show a decrease. However, the effect of rotation on the needle end-point position in lateral direction is not yet researched, and this is a good indication of targeting precision. Therefore, this work has studied the effect of rotation on the precision of the needle end-point position in lateral direction.

The concept uses pneumatically actuated stepper motors for the needle insertion. As the air will be supplied from outside the MRI room, the maximum frequency of air supply is estimated at 10 Hz. Therefore, the effect of an actuation frequency of 10 Hz on the precision of the needle end-point position in lateral direction is studied as well.

Both effects are researched by inserting a needle in a gelatin phantom at different angular velocities and at continuous versus discrete actuation. It is found that rotation significantly decreases the standard deviation in 6 of the 12 cases. The actuation frequency of 10 Hz does not significantly increase the standard deviation in 7 of the 8 cases. These results can be used to further increase the precision of a biopsy robot, whether it is for breast biopsy or another application.

PREFACE

For the past eight months, I have worked on this thesis. What I really enjoyed about it was the variety of the project. I was able to combine many different aspects of mechanical engineering: concept generation, computer-aided design, programming, dynamics and statistics, but also building an experimental setup and getting the stepper motors to work the way they should. Especially these last two parts were unfamiliar and challenging to me, and I liked gaining new knowledge and skills in these areas. I am lucky to have found a thesis subject that interests me this much, and I have enjoyed generating new knowledge for the medical robotics field. In reaching this result, I have had the help and support of many people, and I want to thank some in particular.

I am very grateful that I could do this thesis for Demcon with the supervision of Michiel Plooi. Our meetings were very helpful to me, and I always felt more motivated afterwards. Outside of our regular meetings, I still felt that I could ask for advice when needed. I have learned a lot from you and could not have wished for a better supervisor. I also want to thank Pieter Wiskerke for allowing me this opportunity and for helping define the direction of the thesis.

Next, I want to thank John van den Dobbelsteen for his supervision in this project and helping me by providing testing facilities at the Delft University of Technology. You gave me new insights and helped me to keep the clinical relevance of this project in mind. I also want to thank Jan van Frankenhuyzen for his help with 3D printing and for his insights when I was building the setup.

Furthermore, I want to thank my friends who I studied with during this project, especially Bram Haanen and Maxine Rietveld. Our coffee and lunch breaks have helped me to stay motivated and made the process more fun. Furthermore, Bram, thank you for proofreading my entire work when you were also in the final stages of your thesis, I really appreciate it.

I also want to thank my roommates for their support and interest in my thesis. I am also thankful that when my room flooded in the week of my green light, you have taken care of this, allowing me to focus on finalizing my thesis.

Finally, I want to thank my family and Sybren Heikens. You have always undoubtedly believed in me and given me the support I needed. And Sybren, thank you for proofreading everything, for your advice and for cheering me up.

Laurence Koopman, August 2021

CONTENTS

1	INTRODUCTION	1
1.1	Background	1
1.2	State of the art	2
1.3	Goal	3
1.4	Thesis outline	3
2	METHODS	5
2.1	Hypotheses	5
2.2	Experiment	6
2.3	Phantom	7
2.3.1	Fabrication	7
2.4	Experimental setup	7
2.4.1	Design	8
2.4.2	Actuation	8
2.4.3	Control	8
2.5	Protocol	8
2.6	Data collection	9
2.7	Analysis method	9
3	RESULTS	11
3.1	Continuous actuation	11
3.2	Actuation at 10 Hz	12
3.3	Actuation at 5 Hz	14
4	DISCUSSION	17
4.1	Interpretation of results	17
4.1.1	Research question 1: What is the effect of rotation on the deviation of needle end-point position in lateral direction in gelatin?	17
4.1.2	Research question 2: What is the effect of a 10 Hz actuation frequency on the deviation of needle end-point position in lateral direction in gelatin?	18
4.1.3	Actuation at 5 Hz	18
4.1.4	Clinical relevance of the results	19
4.1.5	Precision and accuracy	19
4.1.6	Order of experiments	19
4.1.7	Difference in x and y standard deviation	19
4.1.8	Relation to similar studies	19
4.2	Limitations	20
4.3	Future recommendations	21
5	CONCLUSION	23
A	CONCEPT	27
B	EXPERIMENTAL SETUP DETAILS	31
C	ARDUINO CODE	33
D	ELECTRONICS WIRING	35
E	MATLAB CODE	37
F	STANDARD DEVIATION	41

LIST OF FIGURES

Figure 1.1	Sunram 5, a needle positioning robot with pneumatic stepper actuation by [Groenhuis et al., 2020]	2
Figure 2.1	Two types of cutting tips	6
Figure 2.2	The experimental setup, with indication of x, y and z axis . . .	6
Figure 2.3	The experimental setup with the most important features labeled: 1. damping mat 2. linear stage 3. rotation motor 4. motor to needle connection 5. needle 6. needle guidance 7. container with gelatin phantom 8. transparent plate for calibration 9. camera holder	8
Figure 3.1	Needle end-point coordinates in one layer of gelatin for continuous actuation	11
Figure 3.2	Standard deviation of needle end-point for continuous actuation. Statistically significant differences in variance with respect to 0 rpm are indicated with an asterisk in the colour of the coordinate	12
Figure 3.3	Standard deviation of needle end-point for 10 Hz actuation . . .	13
Figure 3.4	Standard deviation of needle end-point comparing continuous actuation with 10 Hz. Statistically significant differences in variance with respect to 0 rpm are indicated with an asterisk in the colour of the coordinate	14
Figure A.1	Concept 1	28
Figure A.2	Concept 2	28
Figure A.3	Concept 3, image from [Thang, 2016]	28
Figure A.4	SolidWorks model of the concept for an magnetic resonance imaging (MRI)-compatible needle insertion mechanism	29
Figure C.1	The Arduino code for 120 rpm at continuous actuation	33
Figure C.2	The Arduino code for 120 rpm at 10 Hz actuation	34
Figure D.1	The wiring for the electronics	35
Figure F.1	Standard deviation	41

ACRONYMS

CT	computed tomography	1
MRI	magnetic resonance imaging	xi
US	ultrasound	1

1.1 BACKGROUND

In 2020, 19.3 million people were diagnosed with cancer [WHO, 2021a]. For certain types of cancer, such as breast cancer, the concluding diagnosis is obtained by taking a biopsy of the lesion. A physician takes the biopsy by manual insertion of a needle. The physician makes and executes a plan to approach the lesion with the use of and often guided by imaging techniques such as ultrasound (US), computed tomography (CT) or MRI. However, there are several reasons why taking a biopsy accurately can be challenging. First of all, several organs can move due to respiration ([Wagman et al., 2003], [Wysocka et al., 2010], [Bryan et al., 1984], [Kubo and Hill, 1996], [Mageras, 2001], [Davies et al., 1994], [Lang et al., 2006] and [Qi et al., 2010]), and therefore, the lesion moves as well, making the procedure more challenging. The second contributing factor to possible errors in the procedure is that humans are prone to errors and inconsistency [Podder et al., 2005]. Furthermore, the trajectory towards the lesion often involves “tissue heterogeneity, anisotropy, nonlinear viscoelasticity, relaxation, tissue deformation and deflection, unfavorable anatomic structures, needle bending, inadequate sensing, and poor maneuverability” [Podder et al., 2005], which makes needle insertion complex. Therefore, a physician could miss the target during needle insertion. If the target is missed, the procedural time will increase, and healthy surrounding tissue is damaged. For a CT-guided procedure, any additional CT-scans for following attempts will result in further radiation exposure. Therefore, it is essential to ensure that the biopsy needle reaches the target at the first attempt. A robotic system could improve the precision and accuracy of the currently manually performed procedure.

Amongst all cancer types, breast cancer is the worlds most prevalent type [WHO, 2021b]. MRI is often used for breast biopsy imaging, as it can visualize the soft tissue precisely [Shimizu et al., 2000]. However, an MRI-compatible system should not contain metallic, magnetic or electrically conductive materials [Yakar et al., 2011]. Classical robots generally contain these materials.

There are two primary challenges in robotic breast biopsy: the restrictions brought along by MRI and targeting precision and accuracy. The precision and accuracy is sufficient when the lateral deviation is below 1 mm. This is required to reach even small-size (3 mm, [VanSonnenberg et al., 1988]) lesions. To approach this problem, a concept (Appendix A) was developed to insert the needle while rotating the needle along the translation axis. One actuator is used for both the rotation and translation of the needle, which are thus coupled. The mechanism is actuated with a pneumatic stepper motor, and the air is supplied from outside the MRI-room so that no metallic, magnetic or electrically conductive materials are required inside the MRI room. Pneumatic actuation will require air supply tubes of approximately 5 m long. With tubes of this length, a frequency of 10 Hz is realistic [Groenhuis and Stramigioli, 2018].

[Groenhuis et al., 2020] have developed a pneumatically actuated MRI-safe biopsy robot for needle positioning, as can be seen in Figure 1.1. This robot makes use of pneumatic stepper motors with air supply from outside the MRI-room as well,

resulting in similar frequencies as described previously. The results of this needle positioning robot are very promising, and therefore it is important to research the possibilities for needle insertion as well.



Figure 1.1: Sunram 5, a needle positioning robot with pneumatic stepper actuation by [Groenhuis et al., 2020]

1.2 STATE OF THE ART

To achieve a high precision and accuracy (of less than 1 mm lateral deviation), several approaches are presented in literature.

The effects of the needle tip geometry have been researched for a bevel, cone and triangular tip ([O’Leary et al., 2003] and [Okamura et al., 2004]). A triangular tip is found to have the least resistance force, followed by bevel and then cone. A bevel tip is more susceptible to changes in the material and deflects more than the other two tip geometries. A smaller needle diameter has less resistance force but more deflection.

Substantial research has been conducted on needle insertion forces ([O’Leary et al., 2003], [Okamura et al., 2004], [Kobayashi et al., 2008], [Yang et al., 2018], [Abolhassani et al., 2007] and [Kobayashi et al., 2009]). With this knowledge, the needle can be modelled to stop at the target more accurately [Simone and Okamura, 2002].

Regarding the insertion technique, research ([Abolhassani et al., 2006], [Abolhassani et al., 2007] and [Badaan et al., 2011]) was conducted studying the effect of rotating a needle along its insertion axis, and this was found to “reduce tissue indentation before puncture and frictional forces after puncture” [Abolhassani et al., 2006]. [Badaan et al., 2011] researched the effect of needle rotation on target displacement and found that “needle rotation may be an effective method of reducing targeting errors.”

The principle of rotating the biopsy needle along the insertion axis has great potential in improving the precision and accuracy of a biopsy robot. Therefore, this technique is applied in the concept described in Section 1.1 with the aim of achieving a lateral deviation of below 1 mm.

1.3 GOAL

This thesis will research two relevant questions. First of all, the concept described in Section 1.1 rotates the needle along the insertion axis, intending to improve the precision and accuracy. Research in literature studies the effect of needle rotation on insertion force, tissue indentation and axial displacement of the target, but not on needle end-point deviation in lateral direction. The latter will indicate whether the targeting precision and accuracy increases or not. Therefore, it is important to research the effect of rotation on the needle end-point position standard deviation. Furthermore, the concept uses a pneumatic stepper motor, which will have a frequency of around 10 Hz. This is a relatively low frequency, and if an angular velocity of around 60 rpm is desired, this will result in a step size of 36 degrees. This is relatively large. Therefore, it is important to research the effect of such a frequency and associated step size on the needle end-point position standard deviation. This results in the following research questions:

- What is the effect of rotation on the deviation of needle end-point position in lateral direction in gelatin?
- What is the effect of a 10 Hz actuation frequency on the deviation of needle end-point position in lateral direction in gelatin?

The first research question will give more insight into whether using rotation is a suitable method for increasing the precision of needle insertion. The second question will give insight into whether using a pneumatic stepper motor at 10 Hz would be a feasible solution or if the frequency will result in a too large (above 1 mm) deviation of the needle end-point.

1.4 THESIS OUTLINE

The thesis is structured as follows. The experiment of this research is described in Chapter 2. Here, the hypotheses, the experiment, the phantom and the experimental setup used for the experiments are described, as well as the protocol, the data collection and analysis method. In Chapter 3, the results of the experiment are presented. Chapter 4 interprets the results, discusses the limitations of this work and gives recommendations for future work. Finally, Chapter 5 gives a conclusion of the thesis.

2 | METHODS

This chapter will describe the experiment that has been conducted to answer the research questions stated in Section 1.3. First, the hypotheses for the experiment are presented in Section 2.1. The experiment is described in Section 2.2. The fabrication and properties of the phantoms used for the experiments are described in Section 2.3. Next, the experimental setup, including design, actuation and control, is presented in Section 2.4. The protocol of the experiment is described in Section 2.5. Next, the data collection approach is given in Section 2.6. Finally, the analysis method is described in Section 2.7.

2.1 HYPOTHESES

The experiment is designed to answer the following research questions:

- What is the effect of rotation on the deviation of needle end-point position in lateral direction in gelatin?
- What is the effect of a 10 Hz actuation frequency on the deviation of needle end-point position in lateral direction in gelatin?

For the first question, it is expected that rotation will decrease the deviation in needle end-point because of two reasons. First, the work of [Badaan et al., 2011] found that rotation reduces target displacement in axial direction. The work of [Abolhasani et al., 2006] found that rotation reduces tissue indentation and frictional forces after puncture. Although these are different parameters than the needle end-point in lateral direction, it is expected that this will also have a reduced value, as the frictional force acting on the needle reduces due to rotation. Second, as the needle has a diamond tip (see Figure 2.1a), the different cutting edges are expected to improve indentation when the needle is rotated. This principle can be compared to the indentation made by the tip of a drill. Here, rotation is also used to let the chisel edge and cutting lips (see Figure 2.1b) cut through the material and thereby improve indentation [Roukema, 2006]. Furthermore, [Okamura et al., 2004] have studied the effect of needle tip geometry on cutting force, and found that a triangular tip has a significantly lower axial force than a bevel or conical tip. A triangular tip has more sharp edges than the other two types. [Okamura et al., 2004] state that the amount of sharp edges correlates with the ease of crack propagation and therefore, the cutting force, thus explaining the lower cutting force for a triangular tip. It is expected that rotation will increase the ease of cutting with the diamond tip needle further, similar to drilling. Therefore, because of the expected improved indentation due to rotation, the needle is predicted to deflect less in the lateral direction when rotation is included.

Concerning the second research question, it is expected that a frequency of 10 Hz will increase the deviation. The needle will not rotate continuously, but in discrete steps. After each rest, when the needle starts to move again, there is a peak in friction expected because the needle has to overcome static friction, which generally has a higher friction coefficient than dynamic friction. Because of this peak in frictional force acting on the needle, the needle is expected to deflect slightly. A slight increase in deviation is also expected because of the motor's and coupling's inertia.

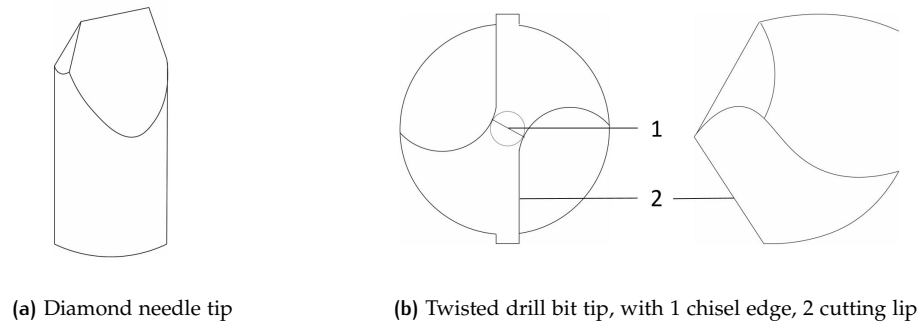


Figure 2.1: Two types of cutting tips

2.2 EXPERIMENT

This section describes the experiment, as shown in Figure 2.2, that rotates a needle along the insertion axis, which is indicated as the z axis. A linear guidance is actuated by a stepper motor, inserting the needle. On the translation platform, a stepper motor is mounted, providing the rotation. A diamond-shaped 20 Gauge needle is attached to the stepper motor, which can thus separately rotate around its own axis while being inserted. The needle is inserted in a transparent container with gelatin in it, mimicking breast tissue. The needle is inserted until the end of the gelatin, which is a length of 90 mm through gelatin. At the end of the container, a photo is taken, from which the needle end-point coordinates (x and y as indicated in Figure 2.2) in lateral direction are determined.

All testing conditions are listed in Table 2.1. The linear velocity is 5 mm/s in every experiment. The angular velocity is varied, ranging from 0 to 120 rpm in steps of 30. The experiments are executed at both "continuous" actuation frequency, meaning using the step size of 1.8 deg of the motors, as well as at 10 Hz actuation frequency, where a longer delay is put between several steps, resulting in a frequency of 10 Hz. The 10 Hz is done to mimick the effect of a pneumatic stepper motor. The experiment is executed at 5 Hz for only one testing condition to give an indication of the effect of lower frequencies.

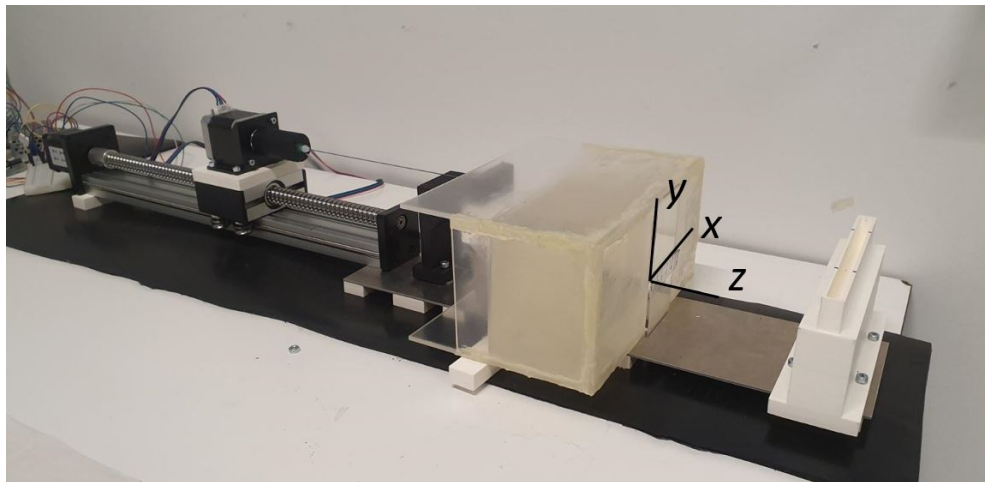


Figure 2.2: The experimental setup, with indication of x , y and z axis

Angular velocity in rpm	Actuation frequency	One layer of gelatin	Two layers of gelatin
0	"continuous"	✓	✓
	10 Hz	✓	✓
30	"continuous"	✓	✓
	10 Hz	✓	✓
60	10 Hz	✓	✓
90	"continuous"	✓	✓
	10 Hz	✓	✓
120	"continuous"	✓	✓
	5 Hz	✓	-
	10 Hz	✓	✓

Table 2.1: Table with testing conditions of the experiment. The linear velocity is always 5 mm/s. "Continuous" refers to actuation in steps of 1.8 degrees with no additional delay

2.3 PHANTOM

A gelatin phantom is used, mimicking breast tissue. This is a common material for a soft tissue biopsy phantom [Leibinger et al., 2016], with the added advantage that it is transparent. Transparency is required for the measurement method, which makes photos of the needle end-point. Although breast tissue is heterogeneous and gelatin results in a homogeneous substance, the homogeneous property allows equal comparison of measurements. The needle is always inserted in a new part of the gelatin, so that the material remains cohesive. The fabrication of the phantom is described in the subsection that follows.

2.3.1 Fabrication

The phantom is made from Dr. Oetker porcine leaf gelatin. The gelatin leaves are put in water for 5 minutes and then added to new water and heated below boiling temperature, until the leaves are completely dissolved. Then, the gelatin is placed in the container in a refrigerator to set overnight. For the one layer of gelatin phantom, 18 leaves are used for 1.5 L of water. The two-layered gelatin phantom has the same volume, but different concentrations of gelatin. The back layer consists of 12 gelatin leaves in 0.75 L, and the front layer of 8 leaves in 0.75 L, creating a difference in stiffness between the layers.

The one layer phantom was used for initial testing. Next, the two layer phantom was used. In real biopsy, the needle will move through layers of different stiffness and therefore, this phantom is considered a more realistic and also a more challenging testing medium. Each gelatin sample was prepared in the same manner, but a small difference in temperature, cooling time or water volume could lead to a small variation in stiffness of the gelatin. However, these differences are expected to be insignificant and therefore, the measurements conducted in different gelatin samples are compared with each other.

2.4 EXPERIMENTAL SETUP

This section will present the design of the experimental setup (Section 2.4.1) including the most important features of it. The actuation (Section 2.4.3) and control (Section 2.4.3) of the setup are separately described.

2.4.1 Design

The experimental setup is shown in Figure 2.3. The most important features of the setup are numbered, and all nine features will be briefly described here. First, the stepper motors require damping, which is done using a rubber mat (1). Next, the translation of the needle is provided by a linear stage (2), which was purchased as a whole and has 300 mm travel length. The guidance is actuated by a stepper motor. On top of the linear stage, the rotation of the needle is provided by another stepper motor (3). Both stepper motors are further described in Section 2.4.2. The needle is connected to the stepper motor with a 3D printed part (4), which has nearly symmetric inertia and a small slit, which provides tolerance for misalignment. The needle (5) is 20 Gauge, 200 mm length with a diamond-shaped tip. Next, the needle is guided by a 3D printed needle guidance (6), to prevent the needle from deflecting under its own weight and to align the needle in a straight manner. Then, the needle enters the gelatin, which is in a transparent container (7) of lasercut PMMA plates glued together. Behind the container is a transparent PMMA plate (8), with two 50 mm rulers for spatial calibration on it. These are oriented in x and y direction, which is perpendicular to the needle axis, as is indicated in Figure 2.2. Finally, a camera holder (9) is positioned behind the setup, where a mobile phone camera is placed to take photos of the needle endpoint. More details concerning parts can be found in Appendix B.

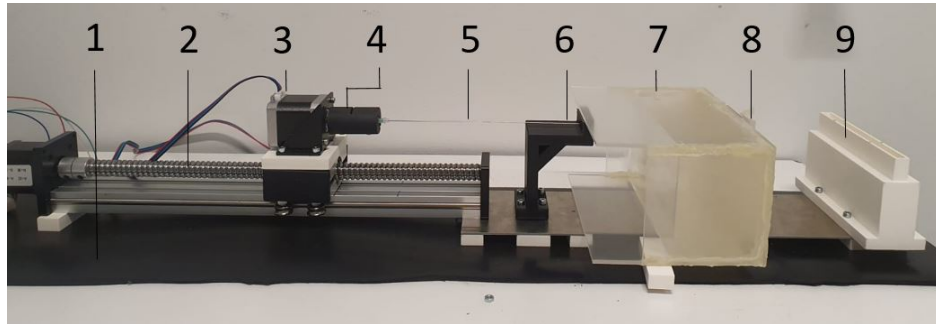


Figure 2.3: The experimental setup with the most important features labeled: 1. damping mat 2. linear stage 3. rotation motor 4. motor to needle connection 5. needle 6. needle guidance 7. container with gelatin phantom 8. transparent plate for calibration 9. camera holder

2.4.2 Actuation

The setup is actuated by two NEMA 17 stepper motors. These both have a step size of 1.8 degrees. Each motor has its own power supply (12 V) and driver (DRV8825) to ensure that no steps are skipped.

2.4.3 Control

The setup is controlled with one Arduino Uno that controls both stepper motors. Coding in Arduino determines the rotational velocity and frequency of both stepper motors. The coding and wiring for the control can be found in Appendix C and Appendix D, respectively.

2.5 PROTOCOL

Preparation: The gelatin container is prepared a day before testing. On the morning of testing, the container is removed from the refrigerator. Any fog on the container

is removed with a tissue for a clearer image of the needle end-point. The container is placed on the experimental setup, with the back against the transparent calibration plate. The phone camera is placed in the camera holder. Then, the proper Arduino code for a specific test condition is selected. It is visually confirmed that the platform is in its initial position. The power supplies for both stepper motors are plugged into a power strip with an on/off switch, first turned off.

Execution: The Arduino code is set to forward actuation. Once uploaded, the power supply is switched on. Then, the needle moves forward for the specified distance. After the distance is travelled, there is a delay in code. In this period, the power supply is switched off. A photo is taken of the needle position and labelled with its measurement number. Next, the code is changed to backward and uploaded. Again, once uploaded, the power supply is switched on. When the specified distance is travelled and the platform is in its initial position, there is another delay, during which the power supply is switched off. The gelatin container is moved in the x -direction, so that the next insertion will use a new part of the gelatin. The execution steps are repeated until 17 measurements are conducted for one test condition. The steps can be repeated for another test condition in new parts of the same gelatin. The gelatin container can also be turned upside down for new parts of the gelatin. One phantom can yield 4 measurements of each 17 insertions, after which a new phantom is made. To ensure that the order of testing does not influence the results, the first two experiments are conducted again in opposite order with a new needle.

2.6 DATA COLLECTION

Data is collected by a mobile phone camera (Samsung S10e, 1.4 μm resolution). When the needle has moved to the end of the gelatin container, the camera takes a photo of the needle end-point. Two rulers of each 50 mm are placed on a transparent plate against the gelatin container. One ruler is placed horizontally and the other one vertically, representing the x and y axis. These are used for spatial calibration. Every test condition is repeated 17 times. The camera does not move within one test condition and the measurements are always calibrated per test condition for image processing.

2.7 ANALYSIS METHOD

For each test condition (which has 17 photos), the first photo is used for spatial calibration. The photo is converted to a 50 by 50 mm image in Matlab R2018b, using the rulers that are attached on the plate for calibration. Next, the needle end-point position is determined using `ginput`. This results in an x and y coordinate of the needle. From the coordinates, the standard deviation and variation per measurement set are calculated. The needle coordinates are also visualised in a plot.

A two-sample F-test is used to determine whether the difference in variance is statistically significant. This test compares two samples. The null hypothesis is that the data vectors have equal variance, and the alternative hypothesis is that the variance of the two samples is not equal. If $h = 1$, the null hypothesis is rejected at the 5% significance level ($\alpha = 0.05$). The p -value represents "the probability of observing a test statistic as extreme as, or more extreme than, the observed value under the null hypothesis" [Mathworks, 2021]. For the continuous actuation, both the x and y data for one and two layers for each angular velocity is compared to the no rotation data, to study the effect of rotation. For the 10 Hz actuation, the x and y data for one

and two layers for each angular velocity, including no rotation, are compared to the data of continuous actuation, to study the effect of the 10 Hz actuation frequency. The 5 Hz data is compared to the continuous and 10 Hz actuation data. Finally, the difference between x and y data for each measurement is compared to determine whether there is a statistically significant difference between the x and y variance. The coding for analysis can be found in Appendix E.

3 | RESULTS

This chapter will present the results of the experiments described in Chapter 2. First, the results of the "continuous" actuation will be presented in Section 3.1 for both one and two layers of gelatin. Next, the results for actuation at 10 Hz actuation will be presented in Section 3.2. Finally, the results for actuation at 5 Hz actuation are presented in Section 3.3. The standard deviation data can be found in Appendix F.

3.1 CONTINUOUS ACTUATION

The effect of rotation is visualised in Figure 3.1. Here, the end-point coordinates are plotted for 120 rpm and no rotation. It can be observed that the needle end-points for rotation are closer together. The experiments for 120 rpm and no rotation in one layer of gelatin are repeated in opposite order with a new needle, to ensure that the order of testing does not influence the results. Similar results were found.

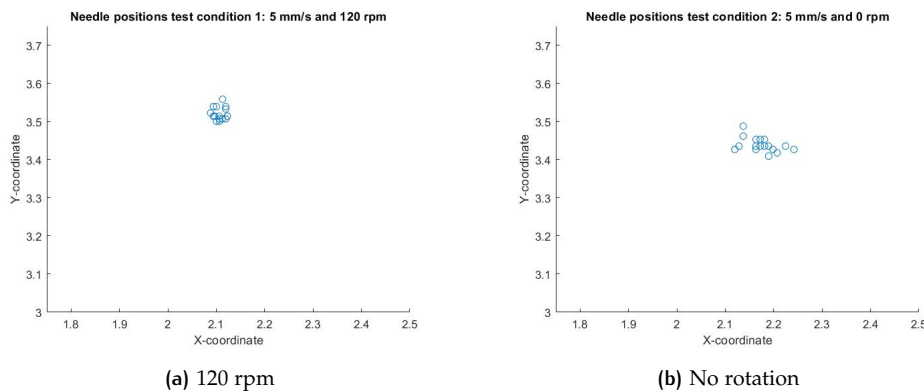


Figure 3.1: Needle end-point coordinates in one layer of gelatin for continuous actuation

Next, the standard deviation of x and y coordinate for different angular velocities in one and two layers of gelatin is plotted in Figure 3.2. It should be noted that there is no value for 60 rpm. For most conditions, the x coordinate has a larger standard deviation than the y coordinate. When considering x and y separately, no rotation has a larger standard deviation for each condition than rotation. However, there seems to be no clear preference for a specific angular velocity within these measurements.

Furthermore, the difference between rotation and no rotation has been evaluated with a two-sample F-test for variance. Data for rotation in one (Table 3.1) and two (Table 3.2) layers has been compared to no rotation. Finally, the difference in variance between x and y for each measurement is tested for statistical significance in Table 3.3.

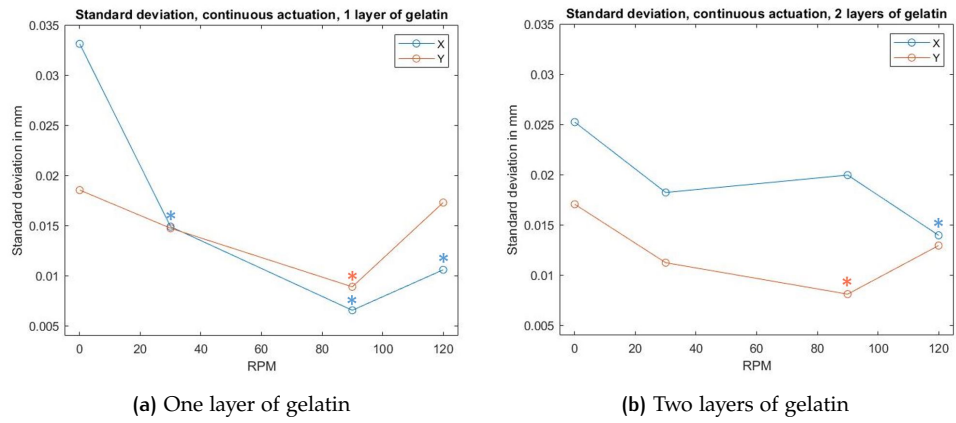


Figure 3.2: Standard deviation of needle end-point for continuous actuation. Statistically significant differences in variance with respect to 0 rpm are indicated with an asterisk in the colour of the coordinate

Angular velocity in rpm	coordinate	h	p-value
120	x	1	$< \alpha$
	y	0	7.931e-01
90	x	1	$< \alpha$
	y	1	$< \alpha$
30	x	1	$< \alpha$
	y	0	4.444e-01

Table 3.1: Two-sample F-test for variance, for continuous actuation in one layer of gelatin, compared to no rotation. α is 0.05

Angular velocity in rpm	coordinate	h	p-value
120	x	1	$< \alpha$
	y	0	8.222e-01
90	x	0	3.701e-01
	y	1	6.1e-03
30	x	0	2.039e-01
	y	0	1.049e-01

Table 3.2: Two-sample F-test for variance, for continuous actuation in two layers of gelatin, compared to no rotation. α is 0.05

Angular velocity in rpm	layers	h	p-value
120	1	0	6.66e-02
	2	0	5.123e-01
90	1	0	2.325e-01
	2	1	$< \alpha$
30	1	0	9.725e-01
	2	0	6.13e-02
0	1	1	$< \alpha$
	2	0	1.273e-01

Table 3.3: Two-sample F-test for variance, for continuous actuation, comparing the variance between x and y . α is 0.05

3.2 ACTUATION AT 10 HZ

First, the standard deviation of the x and y coordinate for different angular velocities in one and two layers of gelatin at 10 Hz is presented in Figure 3.3.

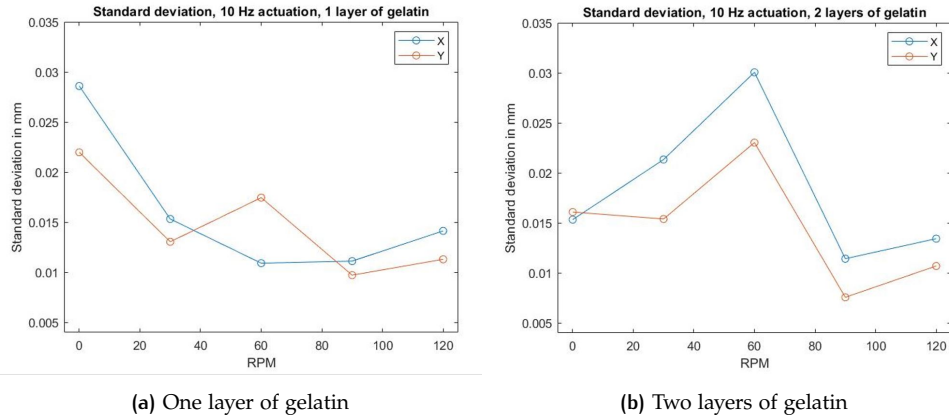


Figure 3.3: Standard deviation of needle end-point for 10 Hz actuation

Next, 10 Hz is compared to continuous actuation. Each standard deviation is plotted separately: for x and y coordinate and for one and two layers. The results can be observed in Figure 3.4. In most cases, 10 Hz has a high standard deviation around 60 rpm, although the standard deviation for continuous actuation for 60 rpm is unknown. For the other conditions, 10 Hz has a comparable standard deviation to continuous actuation.

Furthermore, the two-sample F-test evaluates the significance of the differences in variance. Data for 10 Hz actuation for one (Table 3.4) and two (Table 3.5) layers of gelatin is compared to continuous actuation. The difference between the x and y variance is evaluated for each measurement in Table 3.6.

Angular velocity in rpm	coordinate	h	p-value
120	x	0	2.694e-01
	y	0	1.018e-01
90	x	1	$< \alpha$
	y	0	7.249e-01
30	x	0	9.457e-01
	y	0	6.410e-01
0	x	0	5.646e-01
	y	0	5.026e-01

Table 3.4: Two-sample F-test for variance, for 10 Hz actuation in one layer of gelatin, compared to continuous actuation. α is 0.05

Angular velocity in rpm	coordinate	h	p-value
120	x	0	9.772e-01
	y	0	1.310e-01
90	x	1	$< \alpha$
	y	0	7.886e-01
30	x	0	5.461e-01
	y	0	2.375e-01
0	x	0	5.44e-02
	y	0	8.201e-01

Table 3.5: Two-sample F-test for variance, for 10 Hz actuation in two layers of gelatin, compared to continuous actuation. α is 0.05

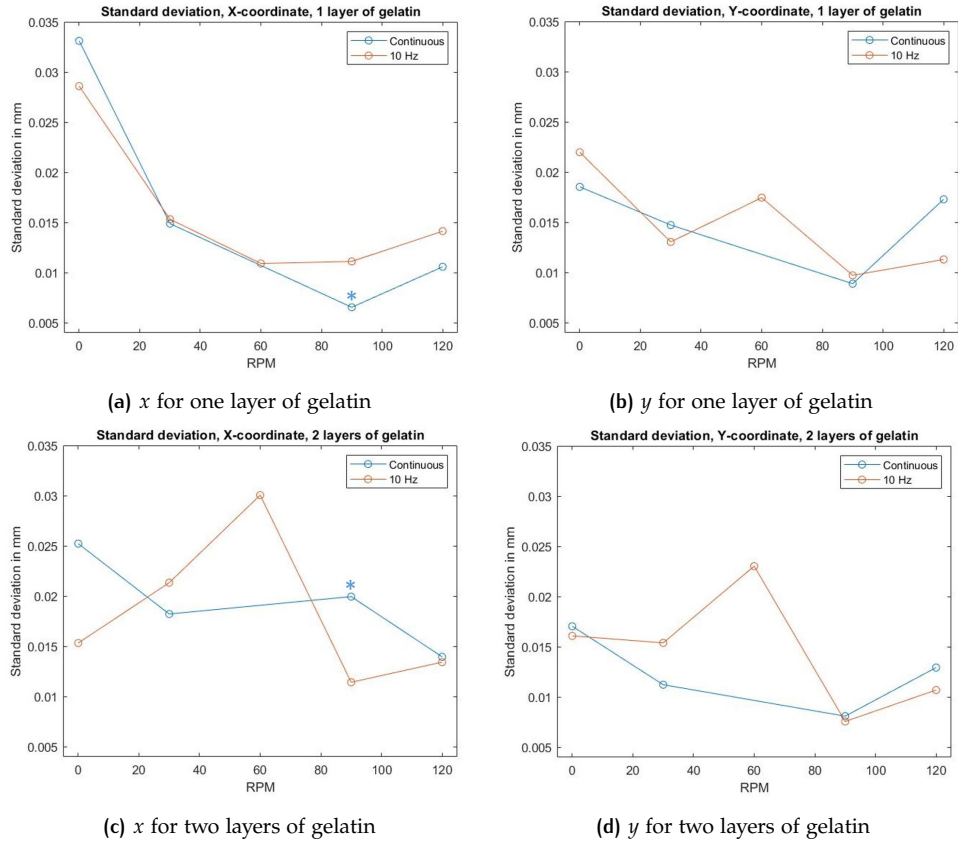


Figure 3.4: Standard deviation of needle end-point comparing continuous actuation with 10 Hz. Statistically significant differences in variance with respect to 0 rpm are indicated with an asterisk in the colour of the coordinate

Angular velocity in rpm	layers	h	p-value
120	1	0	3.797e-01
	2	0	3.727e-01
90	1	0	5.960e-01
	2	0	1.096e-01
60	1	0	6.91e-02
	2	0	2.972e-01
30	1	0	5.276e-01
	2	0	2.719e-01
0	1	0	3.025e-01
	2	0	8.492e-01

Table 3.6: Two-sample F-test for variance, for 10 Hz actuation, comparing the variance between x and y . α is 0.05

3.3 ACTUATION AT 5 HZ

One experiment was conducted to study the effect of 5 Hz. This was conducted at 120 rpm in one layer of gelatin. The standard deviation of this experiment can be found in Table 3.7. In the y direction, the standard deviation is lowest for 5 Hz and highest for continuous. In the x direction, continuous and 5 Hz actuation have a similar standard deviation, that is lower than 10 Hz.

The two-sample F-test evaluates the significance of the differences in variance. Data for 5 Hz actuation in one layer of gelatin is compared to continuous and 10 Hz actuation. The results can be found in Table 3.8. The difference in variance in x and

y is compared as well and the result can be found in Table 3.9.

Actuation	Standard deviation x in mm	Standard deviation y in mm
Continuous	1.06e-02	1.73e-02
5 Hz	1.09e-02	9.21e-03
10 Hz	1.41e-02	1.13e-02

Table 3.7: Standard deviation for 120 rpm in one layer of gelatin for continuous, 5 and 10 Hz actuation

Actuation frequency	coordinate	h	p-value
Continuous	x	0	9.129e-01
	y	1	$< \alpha$
10 Hz	x	0	3.090e-01
	y	0	4.222e-01

Table 3.8: Two-sample F-test for variance, for 5 Hz actuation in one layer of gelatin, compared to continuous and 10 Hz actuation. α is 0.05

Angular velocity in rpm	layers	h	p-value
120	1	0	5.074e-01

Table 3.9: Two-sample F-test for variance, for 5 Hz actuation, comparing the variance between x and y . α is 0.05

4

DISCUSSION

In this chapter, the results of Chapter 3 are interpreted in Section 4.1. Next, the limitations of this work are discussed in Section 4.2. Finally, recommendations for further work are given in Section 4.3.

4.1 INTERPRETATION OF RESULTS

The experiment of this work is conducted to answer two research questions. The results are interpreted regarding the first and second research question in Section 4.1.1 and Section 4.1.2, respectively. Furthermore, the results for actuation at 5 Hz are interpreted in Section 4.1.3. Next, the relevance of the results is discussed in Section 4.1.4. Section 4.1.5 discusses why precision is determined but accuracy could not be determined. Furthermore, the influence of the order of experiments is discussed in Section 4.1.6. Next, the difference in x and y coordinate is discussed in Section 4.1.7. Finally, the work is related to similar studies in Section 4.1.8.

4.1.1 Research question 1: What is the effect of rotation on the deviation of needle end-point position in lateral direction in gelatin?

The effect of rotation on needle end-point deviation in lateral direction is studied. When studying the difference between 120 rpm and no rotation as presented in Figure 3.1, it is clearly visible that rotation results in less deviation, and therefore a more precise insertion. In all cases for continuous actuation (Figure 3.2), rotation results in a decrease of standard deviation compared to no rotation. In 6 of the 12 cases, the difference in variance of rotation versus no rotation is statistically significant. Therefore, the first hypothesis is confirmed.

Similar studies ([Abolhassani et al., 2006], [Badaan et al. 2011]) state the effect rotation has (on friction force, tissue indentation and target displacement), but these studies do not explain *why* rotation could have such effects. This thesis considers the following two explanations for the decrease in standard deviation due to rotation. First, as was mentioned in Section 2.1, rotation is expected to improve indentation and therefore, the needle is expected to deflect less. A second principle is thought to have a contribution to the lower standard deviation as well, although this contribution is expected to be smaller. Therefore, Section 2.1 introduced only the first explanation. The second principle concerns stability, as stability is expected for rotation around the insertion axis. The needle has two identical principal moments and one distinct principal moment. The needle is rotated around the axis with the distinct moment of inertia (the z axis), and rotation around the distinct axis is known to be stable to small perturbations [Bacher et al., 2017]. This is related to stable rotation around the first and third principal moment (in case of three distinct principal moments), which is called the tennis racket theorem [Poinsot, 1851] or the Dzhanibekov effect. This effect is also used for bullets, rugby balls and for some satellite launches, where in all cases the object is rotating around its travel axis (the distinct, first or third axis) to decrease deviation from the path because of the stability around this axis. Small perturbations, such as friction force, are filtered out by the stable rotation. Therefore, the rotation is expected to provide stability

and thus decrease the standard deviation. However, this contribution is expected to be small as the needle has a relatively low moment of inertia. The contribution of the cutting edges is considered a plausible explanation, but to confirm this, further testing should be done. This could be done, for instance, with different needle tips, comparing rotation and no rotation.

Furthermore, the effect of the angular velocity value is interpreted. An increasing angular velocity does not necessarily result in a decrease in standard deviation. Especially at 90 Hz, the standard deviation seems lowest. However, because the standard deviation fluctuates, it cannot be said with certainty that an angular velocity around 90 rpm is the optimal value. The low standard deviation could also be due to properties of this specific setup. It is concluded that rotation has a decreasing effect on standard deviation of needle end-point in lateral direction, but not for a specific angular velocity. This interpretation is also in line with the work of [Abolhassani et al., 2006], which states that for a decrease in tissue indentation, the specific angular velocity does not matter, as long as there is rotation.

4.1.2 Research question 2: What is the effect of a 10 Hz actuation frequency on the deviation of needle end-point position in lateral direction in gelatin?

The second research question concerns the effect of a 10 Hz actuation frequency. First of all, Figure 3.3 shows that at 10 Hz, rotation (excluding 60 rpm) still results in a decrease of standard deviation. Furthermore, when comparing 10 Hz with continuous actuation, there is not a clear increase in standard deviation for all test conditions. The two-sample F-test indicates that in 7 of the 8 cases, the difference in variance between 10 Hz and continuous actuation is not statistically significant. As described in Section 2.1, an increase in standard deviation was expected due to a 10 Hz actuation frequency. This was because of the expected higher static friction that had to be overcome after every step, and because of the motor's and coupling's inertia. It is thus concluded that these factors do not have a significant effect on the standard deviation.

10 Hz shows a peak in standard deviation at 60 rpm, but this cannot be compared to 60 rpm at continuous actuation, as there have been no experiments conducted at this angular velocity. The peak is unexpected and can be attributed to the mechanical behaviour of the motor or measurement inaccuracies, such as inadequate image processing or faulty placement of the camera. Other angular velocities have more promising results, but in determining the optimal angular velocity for 10 Hz actuation frequency, if there is any, further testing is required.

4.1.3 Actuation at 5 Hz

When studying the effect of 5 Hz, it is surprising that this actuation frequency has a lower standard deviation than 10 Hz. The two-sample F-test indicates statistical insignificance for the difference in variance in 3 of the 4 cases. However, this observation is based on one group of experiments for 120 rpm, and therefore, more data will be needed to accept or reject this statement.

4.1.4 Clinical relevance of the results

As the standard deviation is already on the scale of one-hundredth of a mm, and a precision and accuracy of "only" below 1 mm lateral deviation is required, the decrease in standard deviation is not considered clinically relevant. It is expected, still, that the standard deviation will increase when testing in a more challenging medium. Therefore, the positive effect of rotation could play a larger role, possibly in a more clinically relevant range.

4.1.5 Precision and accuracy

Unfortunately, the range of the results is too small to determine accuracy. For this, the needle positions need to be compared to the expected position of the needle, and this depends on the camera angle. It was expected that the standard deviation would be in the range of a tenth of a mm, based on the work by [Badaan et al., 2011]. In this range, the difference due to the camera angle would have been negligible compared to the differences in standard deviation, but with the range being in the one-hundredth mm range, this is not the case and therefore, statements cannot be made about accuracy. However, precision is determined within a group of measurements and because the camera is placed per group, precision can be evaluated.

4.1.6 Order of experiments

To ensure that the needle does not bend after several measurements, the order of the first two experiments (120 rpm and no rotation in one layer) was reversed and conducted with a new needle. Both results showed a decrease in standard deviation for rotation. Therefore, it is concluded that the needle can be used for many experiments without influencing the measurements.

4.1.7 Difference in x and y standard deviation

A difference between the standard deviation of x and y can be seen in Figure 3.2 and Figure 3.3, where in most cases x seems to have a slightly larger standard deviation than y . However, the difference is not statistically significant in 17 of the 19 cases.

4.1.8 Relation to similar studies

Furthermore, the range of these results can be compared to the range of the results from [Badaan et al., 2011]. Their work conducted the experiments in gelatin as well, but the results were on the scale of a tenth of a mm, which is larger than the results here. A similar needle was used, the only difference being that this work has used a slightly thinner needle (18 G in the paper versus 20 G in this work). Three factors are considered to explain the difference in range. First of all, a different metric is measured: this work considers a needle position, while the paper studies a target position. Furthermore, the direction differs and therefore it is possible that axial target displacement, the metric of [Badaan et al., 2011], has a larger range of displacement than needle end-point in lateral direction. Second, [Badaan et al.,

2011] have made targets of gelatin with a higher stiffness that are embedded in gelatin. Since the targets have a higher stiffness, it is possible that the needle initially pushes the target away before making an indentation in the target, thus resulting in a displacement of the target. It is possible that if this thesis includes targets, the needle position could vary more, as the indentation force of the needle increases due to the higher stiffness, resulting in more deviation of the needle. Thirdly, the work of [Badaan et al., 2011] has a resolution of 14 pixels per mm, which is just a little more than one pixel per tenth of a mm. Since their results are on the scale of a tenth of a mm, this resolution is not very high and could therefore result in errors in measurement and therefore, also in a higher range of displacement. For comparison, the resolution in this work is one pixel per 0.014 mm, thus ten times higher.

4.2 LIMITATIONS

This section will describe the seven most important limitations of this work.

First of all, the test medium for the experiments does not fully represent breast tissue. Gelatin is chosen to mimick breast tissue because it allows for equal comparison of measurements and because it is transparent. However, real tissue is heterogeneous. Gelatin has near linear elastic behaviour and a low viscous nature, which is different from real soft tissue [Leibinger et al., 2016]. For the most realistic case, the needle insertion should be performed in a real patient, that is breathing, causing lesion movement. This is not represented by the gelatin phantom used in this work. Although the safety risks involved with human testing are too high for this stage of the work, further stages in this field require more realistic testing.

Next, this work measures the precision of needle insertions. This is a good indication of the effect of rotation and actuation frequencies. However, the accuracy is not studied. This was not possible with the range of standard deviation combined with the design of the setup. Since multiple samples of gelatin are used, the experiments are spread over various days and therefore, the mobile phone camera is placed for each measurement. This placement can cause small differences in the angle of the camera. This difference cannot be neglected compared to the range in standard deviation and therefore the desired position of the needle end-point is not a fixed value for each measurement. Therefore, the real position cannot be compared to the desired position and thus, the accuracy cannot be determined. A possible solution is using a fixed camera with a similar or higher resolution, that can remain in position throughout all testing.

Thirdly, the experiment was attempted at 60 rpm for "continuous" actuation but could not be executed because the rotation-providing stepper motor does not rotate, but only vibrates at this angular velocity. It is expected that 200 Hz, which is the frequency for 60 rpm at continuous actuation, is the eigenfrequency of the motor, causing the severe vibration. This is a common value for stepper motor resonance. The following calculations further show that this is a plausible suggestion. The formula for resonance frequency, from [Jennings, 1996], is as follows:

$$f = \frac{1}{2 \cdot \pi} \cdot \sqrt{\frac{p \cdot M_h}{J_r}} \quad (4.1)$$

Here, f is the resonance frequency [Hz], p is the number of pole pairs, M_h the holding torque [N·m] and J_r the rotor inertia [kg·m²]. The motor has 50 pole pairs

and a holding torque of 0.50 N·m. The rotor inertia is unknown and is calculated by approximating the shape as a cylinder:

$$J_r = \frac{1}{8} \cdot M \cdot d^2 \quad (4.2)$$

The motor is 360 g, and the rotor is estimated to be half of the motor weight. The width of the stepper motor is 42 mm, and the diameter of the rotor is estimated to be 25 mm, which is slightly more than half of the width. This results in an estimated rotor inertia of $1.41e^{-05}$ kg·m². With this value, the resonance frequency is found to be 212 Hz. Considering that the rotor inertia is approximated, a slightly higher rotor inertia would result in a resonance frequency of 200 Hz. Therefore, it is very likely that resonance is the cause of the motor not rotating at 200 Hz, or 60 rpm.

Furthermore, expanding on the previously described limitation, the properties of the motor could influence the measurements. For the 10 Hz actuation, it was possible to conduct experiments for 60 rpm, but these measurements gave a peak in standard deviation, which could be also due to the mechanical behaviour of the motor, and not specifically due to the needle-gelatin interaction at this angular velocity.

The fifth limitation of this work is that the gelatin is damped. The actuation of the experimental setup required damping, and to ensure that the setup is aligned, the rubber mat for damping was placed under the entire setup. This resulted in damping of the gelatin as well, which potentially influenced the measurements, resulting in relatively low standard deviations.

Next, the experiments are conducted for one needle size. Possibly, thinner needles will show larger differences between rotation and no rotation, or thicker needles have more advantage from rotation as those have a larger moment of inertia around the distinct axis.

Finally, the setup has not been built by a professional. Although the setup appears to be well aligned, there could still be small errors due to inexperience or insufficient tools.

4.3 FUTURE RECOMMENDATIONS

This work has determined the precision of needle insertion under different angular velocities and actuation frequencies. Four topics are important to determine and are therefore recommended for further research.

First of all, it is recommended to conduct further experiments in a more challenging medium, such as PVA and, eventually, real tissue. It is expected that the standard deviation will increase for all measurements. These experiments can possibly put the contribution of rotation in a clinically relevant range.

Second, this work has determined the precision for various conditions. As needle insertion requires both precision and accuracy, it is important to study the accuracy for these conditions as well.

Thirdly, only one experiment was conducted for 5 Hz. This showed promising results, but more data is required to confirm whether this actuation frequency is feasible.

The final recommendation is to research the effect of inserting the needle under

an angle. Possibly, this will present larger differences in results. If this indicates a favor for rotation as well, this increases the possible needle insertion paths.

5 | CONCLUSION

This thesis has researched the effect of rotation and a relatively low actuation frequency on the precision of needle insertion for an MRI-guided breast biopsy robot. Experiments are performed to answer the following two research questions: 1. *What is the effect of rotation on the deviation of needle end-point position in lateral direction in gelatin?* and 2. *What is the effect of a 10 Hz actuation frequency on the deviation of needle end-point position in lateral direction in gelatin?* Regarding the first research question, rotating the needle during insertion reduces the needle end-point standard deviation. In the most optimal case, the standard deviation reduces by 80% from $3.31e-02$ mm to $6.55e-03$ mm. The difference in variance is statistically significant in 6 of the 12 cases. Concerning the second research question, in some cases, an increase in standard deviation of the needle end-point position is found. However, this increase is lower than the decrease due to the rotation. Furthermore, the difference in variance is not statistically significant in 7 of the 8 cases.

All errors are in the range of one-hundredth of a millimeter, which is not considered clinically relevant. However, a reduction in error due to needle rotation could still be useful. Regarding the pneumatically actuated stepper motor concept, it would have a precision well within the clinically accepted range. Therefore, this concept can be further developed. Including rotation does not bring along disadvantages, but it has additional advantages such as a decrease in axial displacement of the target. When further recommendations are executed, the concept presented in this thesis can be further developed, as it has the potential to improve the current procedure of MRI-guided breast biopsy or possibly other types of biopsy.

BIBLIOGRAPHY

- Abolhassani, N., Patel, R., and Moallem, M. (2006). Control of soft tissue deformation during robotic needle insertion. *Minimally Invasive Therapy and Allied Technologies*, 15(3).
- Abolhassani, N., Patel, R., and Moallem, M. (2007). Needle insertion into soft tissue: A survey. *Medical Engineering and Physics*, 29(4).
- Bacher, M., Bickel, B., Whiting, E., and Sorkine-Hornung, O. (2017). Spin-It: Optimizing Moment of Inertia For Spinnable Objects. *Communications of the ACM*, 60(8):92–99.
- Badaan, S., Petrisor, D., Kim, C., Mozer, P., Mazilu, D., Gruionu, L., Patriciu, A., Cleary, K., and Stoianovici, D. (2011). Does needle rotation improve lesion targeting? *International Journal of Medical Robotics and Computer Assisted Surgery*, 7(2).
- Bryan, P. J., Custar, S., Haaga, J. R., and Balsara, V. (1984). Respiratory movement of the pancreas: An ultrasonic study. *Journal of Ultrasound in Medicine*, 3(7).
- Davies, S. C., Hill, A. L., Holmes, R. B., Halliwell, M., and Jackson, P. C. (1994). Ultrasound quantitation of respiratory organ motion in the upper abdomen. *British Journal of Radiology*, 67(803).
- Groenhuis, V., Siepel, F. J., and Stramigioli, S. (2020). Sunram 5: A Magnetic Resonance-Safe Robotic System for Breast Biopsy, Driven by Pneumatic Stepper Motors. In *Handbook of Robotic and Image-Guided Surgery*.
- Groenhuis, V. and Stramigioli, S. (2018). Rapid Prototyping High-Performance MR Safe Pneumatic Stepper Motors. *IEEE/ASME Transactions on Mechatronics*, 23(4).
- Jennings, S. (1996). Basic theory of stepping motors.
- Kobayashi, Y., Onishi, A., Watanabe, H., Hoshi, T., Kawamura, K., and Fujie, M. G. (2008). In vitro validation of viscoelastic and nonlinear physical model of liver for needle insertion simulation. In *Proceedings of the 2nd Biennial IEEE/RAS-EMBS International Conference on Biomedical Robotics and Biomechatronics, BioRob 2008*.
- Kobayashi, Y., Sato, T., and Fujie, M. G. (2009). Modeling of friction force based on relative velocity between liver tissue and needle for needle insertion simulation. In *Proceedings of the 31st Annual International Conference of the IEEE Engineering in Medicine and Biology Society: Engineering the Future of Biomedicine, EMBC 2009*.
- Kubo, H. D. and Hill, B. C. (1996). Respiration gated radiotherapy treatment: A technical study. *Physics in Medicine and Biology*, 41(1).
- Lang, N., Dawood, M., Büther, F., Schober, O., Schäfers, M., and Schäfers, K. (2006). Organ movement reduction in PET/CT using dual-gated listmode acquisition. *Zeitschrift für Medizinische Physik*, 16(1).
- Leibinger, A., Forte, A. E., Tan, Z., Oldfield, M. J., Beyrau, F., Dini, D., and Rodriguez y Baena, F. (2016). Soft Tissue Phantoms for Realistic Needle Insertion: A Comparative Study. *Annals of Biomedical Engineering*, 44(8).
- Mageras, G. S. (2001). Fluoroscopic evaluation of diaphragmatic motion reduction with a respiratory gated radiotherapy system. *Journal of Applied Clinical Medical Physics*, 2(4).

- Mathworks (2021). Two-sample F-test for equal variance.
- Okamura, A. M., Simone, C., and O’Leary, M. D. (2004). Force modeling for needle insertion into soft tissue. *IEEE Transactions on Biomedical Engineering*, 51(10).
- O’Leary, M. D., Simone, C., Washio, T., Yoshinaka, K., and Okamura, A. M. (2003). Robotic needle insertion: Effects of friction and needle geometry. In *Proceedings - IEEE International Conference on Robotics and Automation*, volume 2.
- Podder, T. K., Sherman, J., Clark, D. P., Messing, E. M., Rubens, D. J., Strang, J. G., Liao, L., Brasacchio, R. A., Zhang, Y., Ng, W. S., and Yu, Y. (2005). Evaluation of robotic needle insertion in conjunction with in vivo manual insertion in the operating room. In *Proceedings - IEEE International Workshop on Robot and Human Interactive Communication*, volume 2005.
- Poinsot, L. (1851). *Theorie nouvelle de la rotation des corps*. Bachelier.
- Qi, X. S., White, J., Rabinovitch, R., Merrell, K., Sood, A., Bauer, A., Wilson, J. F., Miften, M., and Li, X. A. (2010). Respiratory organ motion and dosimetric impact on breast and nodal irradiation. *International Journal of Radiation Oncology Biology Physics*, 78(2).
- Roukema, J. C. (2006). *Mechanics and dynamics of drilling*. PhD thesis.
- Shimizu, S., Shirato, H., Aoyama, H., Hashimoto, S., Nishioka, T., Yamazaki, A., Kagei, K., and Miyasaka, K. (2000). High-speed magnetic resonance imaging for four-dimensional treatment planning of conformal radiotherapy of moving body tumors. *International Journal of Radiation Oncology Biology Physics*, 48(2).
- Simone, C. and Okamura, A. M. (2002). Modeling of needle insertion forces for robot-assisted percutaneous therapy. In *Proceedings - IEEE International Conference on Robotics and Automation*, volume 2.
- Thang, N. D. (2016). Rotation and translation shaft 1.
- VanSonnenberg, E., Casola, G., Ho, M., Neff, C. C., Varney, R. R., Wittich, G. R., Christensen, R., and Friedman, P. J. (1988). Difficult thoracic lesions: CT-guided biopsy experience in 150 cases. *Radiology*, 167(2).
- Wagman, R., Yorke, E., Ford, E., Giraud, P., Mageras, G., Minsky, B., and Rosenzweig, K. (2003). Respiratory gating for liver tumors: Use in dose escalation. *International Journal of Radiation Oncology Biology Physics*, 55(3).
- WHO (2021a). All cancers fact sheet.
- WHO (2021b). Breast cancer.
- Wysocka, B., Kassam, Z., Lockwood, G., Brierley, J., Dawson, L. A., Buckley, C. A., Jaffray, D., Cummings, B., Kim, J., Wong, R., and Ringash, J. (2010). Interfraction and Respiratory Organ Motion During Conformal Radiotherapy in Gastric Cancer. *International Journal of Radiation Oncology Biology Physics*, 77(1).
- Yakar, D., Schouten, M. G., Bosboom, D. G., Barentsz, J. O., Scheenen, T. W., and Fütterer, J. J. (2011). Feasibility of a pneumatically actuated MR-compatible robot for transrectal prostate biopsy guidance. *Radiology*, 260(1).
- Yang, C., Xie, Y., Liu, S., and Sun, D. (2018). Force modeling, identification, and feedback control of robot-assisted needle insertion: A survey of the literature.

A

CONCEPT

This appendix gives more insight into the concept. First, the morphological chart used to generate the chosen concept is given. Next, the three most promising concepts are presented. Finally, the chosen concept is presented.

The morphological chart gives solutions to the three main functions a concept should include: actuation, transmission and state detection. The morphological chart can be observed in Table A.1.

Subsolution: Subfunction:	1	2	3	4	5	6	7
Actuation	Pneumatic: - Vane - Turbine - Cylinder - Stepper	Hydraulic: - Vane - Turbine - Cylinder - Stepper	Electric	Piezo	Shape Memory Alloy (SMA)	Electro Active Polymer (EAP)	Heat, chemically or light induced
Trans- mission	Belt	Mirrored configurations	Gears	Spindle	Crank	Cardan shaft	Cable
State detection	Feed forward	Optical encoder	Flow sensor				

Table A.1: Morphological chart for concept generation

By combining elements of the morphological chart, concepts are generated. Several concepts were developed. However, before choosing the three most promising concepts, the choice was made for pneumatic stepper actuation and therefore feed forward state detection. This choice was made because pneumatic actuation is MRI-safe and does not introduce dangerous leakages when using sterile air (as opposed to hydraulic actuation). The complicated dynamic behaviour due to the compressibility of air could make position control challenging. However, using stepper actuation eliminates this problem, and furthermore allows feed forward. With this choice clarified, the three most promising are:

- Concept 1: Pneumatic stepper actuation (1), spindle transmission (4) and feed forward state detection (1)
- Concept 2: Pneumatic stepper actuation (1), gears transmission (3) and feed forward state detection (1)
- Concept 3: Pneumatic stepper actuation (1), gears transmission (3) and feed forward state detection (1)

The three concepts can be seen in Figure A.1 - Figure A.3 All concepts are designed to insert a needle while rotating it along the insertion axis. Both concept 1 and 2 have coupled the rotation and translation, which has the advantage that only one actuator is required. However, the manner in which the needle is attached to the gear in concept 2 is expected to be wobbly as it involves a connection part and therefore is expected to have a negative effect on the precision. This is not the case for concept 1. Concept 3 decouples the translation and rotation and therefore requires two actuators. As the rotation and translation can be coupled, only one actuator is needed for both translation and rotation. Therefore, concept 1 is chosen.



Figure A.1: Concept 1

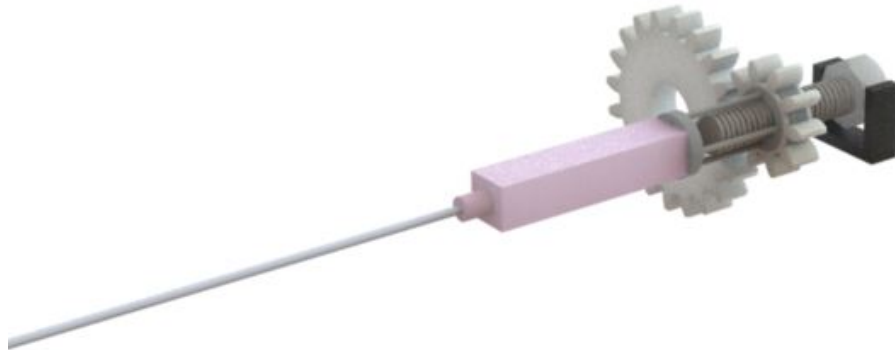


Figure A.2: Concept 2

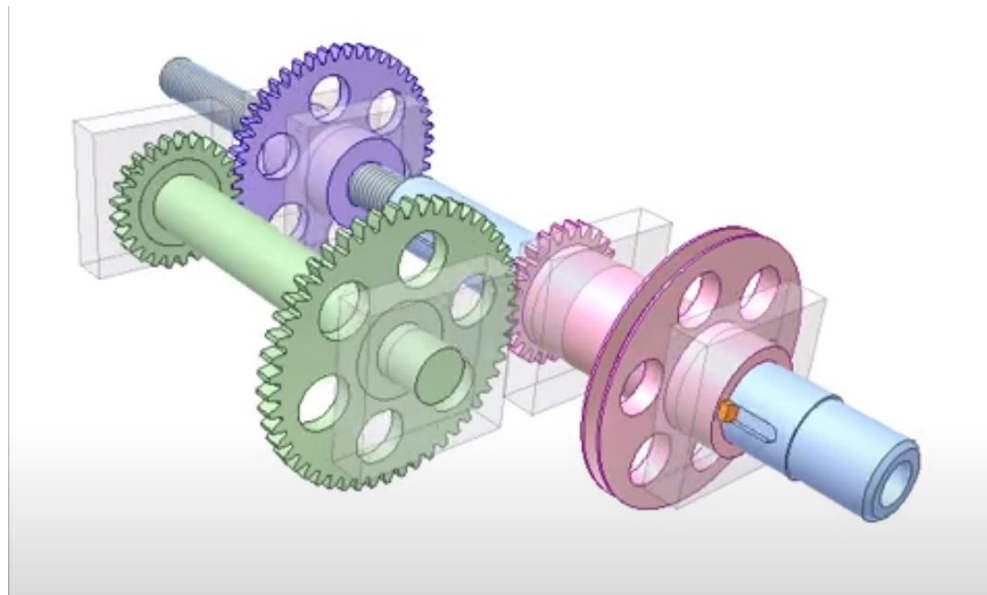


Figure A.3: Concept 3, image from [Thang, 2016]

The concept is actuated by one pneumatic stepper motor. The air is supplied from

outside the MRI-room and the leadscrew and nut will be injection molded or 3D printed, so that no metallic, magnetic or electrically conductive materials are required inside the MRI-room. The transmission is done with a leadscrew, where a nut is clamped and the leadscrew is free to move through the nut. The leadscrew is rotated, thus moving forward through the nut, while also rotating. The needle is attached to the leadscrew, and therefore is rotating and translating, while only the rotation of the leadscrew is actuated. The SolidWorks model is presented in Figure A.4.

The leadscrew has a square thread for less friction and thus higher efficiency. The pitch is initially set to 7.5 mm, because this allows an angular velocity of 40 rpm with a linear velocity of 5 mm/s. The optimal value for the pitch can be adjusted during further development of the concept. Several attempts were made at 3D printing the lead screw and nut, but were not successful yet because the lead screw did not move through the nut. It is recommended to leave sufficient space between the ends of the two parts and to consider effects such as the expanding and contracting of the part due to the printing temperature and cooling down. The orientation of the part during printing will also have an effect on the quality of the print. 3D printing is useful for prototyping purposes, but for commercial production, injection molding or other production techniques can be considered which can achieve a higher part accuracy. However, this decision is left for further work.

Before further developing this concept, two things should be made clear. First of all, whether rotation of the needle will result in a decrease in deviation of the needle. Second, whether using a stepper motor will give sufficient (less than 1 mm standard deviation in lateral direction) precision.

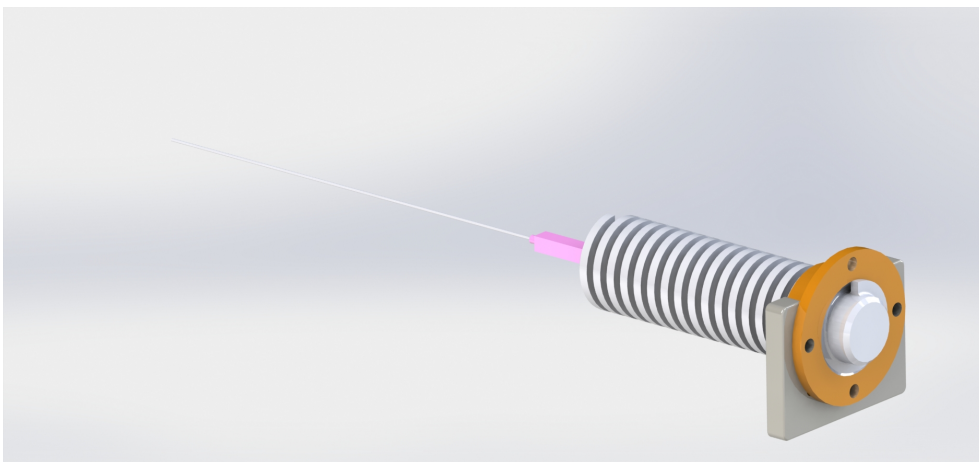


Figure A.4: SolidWorks model of the concept for an MRI-compatible needle insertion mechanism

B | EXPERIMENTAL SETUP DETAILS

All parts used for the experimental setup are specified in alphabetical order.

Part	Function	Description	Supplier
Arduino	Control stepper motors	Arduino Uno	Arduino
Baseplate	Attach all parts to, for alignment	SolidWorks part, Steel	Lasercut
Bracket	Attach stepper motor	NEMA17 ABS bracket	123 – 3d
Breadboard	For electronics		Amazon
Camera holder		SolidWorks part, PLA	3D printed
Driver	Control stepper motors	DRV8825, incl. cooling element	123 – 3d
Linear actuator	Translation of the needle	300 mm, NEMA17, 5 mm pitch	Amazon
Motor–needle coupling		SolidWorks part, PLA	3D printed
Needle		20 G diamond tip, 20 cm	Cook Medical
Needle guidance	Align needle, prevent deflection	SolidWorks part, PLA	3D printed
Plates	Gelatin container	SolidWorks parts, PMMA	Lasercut
Platform	Attach bracket to linear stage	SolidWorks part, PLA	3D printed
Power supply	For stepper motors	12 V	123 – 3d
Rubber mat	Damping the motors	Rubber	MISIT lab
Stepper motor	Rotation of the needle	NEMA17, 1.8 deg step size	123 – 3d
Support blocks	Gelatin container, align height	SolidWorks parts, PLA	3D printed
Wires	Connect motor – breadboard	4-wire cable	123 – 3d

Table B.1: Alphabetical list of parts for the experimental setup

C | ARDUINO CODE

The following Arduino code is used to control the angular velocity, direction and actuation frequency of the two stepper motors. For each specific test condition, the code differs concerning the delays. The code in Figure C.1 illustrates how the motors are controlled for 120 rpm at continuous actuation. Figure C.2 illustrates the code for 120 rpm at 10 Hz actuation. The code is adapted from the tutorial on <https://www.makerguides.com/drv8825-stepper-motor-driver-arduino-tutorial/>.

```
#define dirPinRot 2
#define stepPinRot 4
#define dirPinTrans 7
#define stepPinTrans 8
#define stepsPerRevolution 200 // with 1.8 deg step size, 200 steps result in one
    revolution
void setup() {
    // Declare pins as output:
    Serial.begin(9600);
    pinMode(stepPinRot, OUTPUT);
    pinMode(stepPinTrans, OUTPUT);
    pinMode(dirPinRot, OUTPUT);
    pinMode(dirPinTrans, OUTPUT);
}
void loop() {
    // The spinning direction is set to clockwise:
    digitalWrite(dirPinRot, HIGH);
    digitalWrite(dirPinTrans, HIGH); // LOW = move the linear stage forward, HIGH =
    move the linear stage backward
    delay(3000);
    // One rotation of the linear stage results in 5 mm
    // Spin the stepper motor from the back position to the end of the gelatin
    container, a distance of 120 mm, which is 24 full rotations
    for (int i = 0; i < 24*stepsPerRevolution; i++) {
        // These lines result in 1 linear step and two rotational steps
        // This results in a linear velocity of 5 mm/s (60 rpm) and an angular velocity
        of 120 rpm:
        digitalWrite(stepPinRot, HIGH);
        digitalWrite(stepPinTrans, HIGH);
        delayMicroseconds(1250);
        digitalWrite(stepPinRot, LOW);
        delayMicroseconds(1250);
        digitalWrite(stepPinRot, HIGH);
        digitalWrite(stepPinTrans, LOW);
        delayMicroseconds(1250);
        digitalWrite(stepPinRot, LOW);
        delayMicroseconds(1250);
    }
}
```

Figure C.1: The Arduino code for 120 rpm at continuous actuation

```

#define dirPinRot 2
#define stepPinRot 4
#define dirPinTrans 7
#define stepPinTrans 8
#define stepsPerRevolution 10 // 10 sub-steps result in one step of 18 deg for
    linear and 36 for rotational actuation
#define oneStep 20 // a full revolution uses 20, resulting in 5 mm/s linear velocity
    and 120 rpm for angular velocity
void setup() {
    // Declare pins as output:
    Serial.begin(9600);
    pinMode(stepPinRot, OUTPUT);
    pinMode(stepPinTrans, OUTPUT);
    pinMode(dirPinRot, OUTPUT);
    pinMode(dirPinTrans, OUTPUT);
}
void loop() {
    // The spinning direction is set to clockwise:
    digitalWrite(dirPinRot, HIGH);
    digitalWrite(dirPinTrans, HIGH); //LOW = move the linear stage forward, HIGH =
    move the linear stage backward
    delay(3000);
    // One rotation of the linear stage results in 5 mm
    // Spin the stepper motor from the back position to the end of the gelatin
    container, a distance of 120 mm, which is 24 full rotations of 20 steps
    for (int i = 0; i < 24*stepsPerRevolution; i++) {
        // This loop makes the steps at 10 Hz actuation frequency, as the
        delayMicroseconds + delay(60) adds up to 1.0 second
        for (int j = 0; j < oneStep; j++) {
            // This loop makes the sub-steps
            digitalWrite(stepPinRot, HIGH);
            digitalWrite(stepPinTrans, HIGH);
            delayMicroseconds(500);
            digitalWrite(stepPinRot, LOW);
            delayMicroseconds(500);
            digitalWrite(stepPinRot, HIGH);
            digitalWrite(stepPinTrans, LOW);
            delayMicroseconds(500);
            digitalWrite(stepPinRot, LOW);
            delayMicroseconds(500);
        }
        delay(60);
    }
}

```

Figure C.2: The Arduino code for 120 rpm at 10 Hz actuation

D | ELECTRONICS WIRING

The wiring for the electronics is visualised in Figure D.1. An image of the ports of the driver has been added for clarification. The VMOT and GND ports of the driver are connected to the + and - of the breadboard by two wires each, because using one wire will cause it to heat up too much. The potentiometers on the drivers have been adjusted according to the current limit of the stepper motors, which is 2.5 A. The voltage should be half of the current limit, therefore the voltage was set to 1.25 V. The top stepper motor represents the motor connected to the linear stage, the bottom stepper motor represents the motor connected to the rotation-providing motor. The wiring is adapted from the tutorial on <https://www.makerguides.com/drv8825-stepper-motor-driver-arduino-tutorial/>.

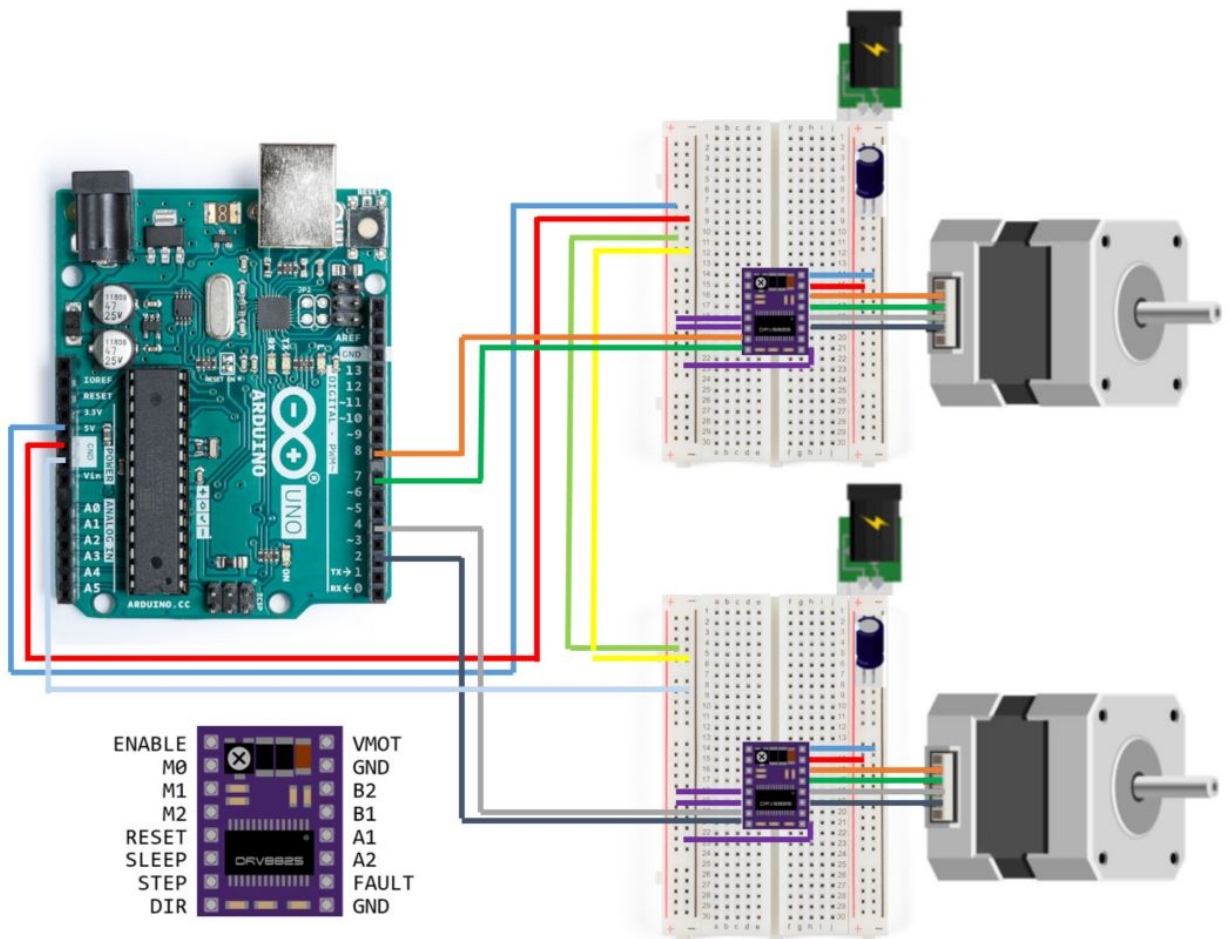


Figure D.1: The wiring for the electronics

E | MATLAB CODE

Here, the four important scripts for data collection and analysis are presented. The spatial calibration and data collection are given for one test condition, as each different test condition uses the same script but adjusted to the filenames. The third script plots the standard deviation. The two-sample F-test script is shortened and presented for continuous actuation in one layer of gelatin, but is similar for other data. The scripts for spatial calibration and data collection are adapted from https://nl.mathworks.com/matlabcentral/answers/uploaded_files/446013/spatial_calibration_demo.m

Listing E.1: Matlab script for spatial calibration

```
1  clc ;
2  close all ;
3  clear all ;
4  workspace ;
5
6  % Load and show the first image for analysis
7  I = imread('H: "Documenten "Studie "Afstuderen "Metingen experiment 1 "5
            mms120rpm10Hz "Measurements21 "5mms120rpm10Hz'1.jpeg ');
8  imshow(I)
9
10 format long g ;
11 format compact ;
12 fontSize = 20 ;
13
14 % Take the grayscale image and show it
15 [rows, columns, numberOfColorBands] = size(I) ;
16 grayscale = rgb2gray(I) ;
17 figureHandle = figure ;
18 subplot(1,2, 1) ;
19 imshow(grayscale, []);
20 axis on ;
21 title('Original Grayscale Image', 'FontSize', fontSize);
22 set(gcf, 'units','normalized','outerposition',[0 0 1 1]);
23 set(gcf, 'name','Calibration','numbertitle','off')
24
25 % Calibrating the image, select the ruler path of 5.00 cm in the image,
26 % this is converted to a value and used for selecting the 5.00 by 5.00 area
27 global lastDrawnHandle ;
28 [cx, cy, rgbValues, xi, yi] = improfile(1000) ;
29 % rgbValues is 1000x1x3. Call Squeeze to get rid of the singleton dimension
    and make it 1000x3.
30 rgbValues = squeeze(rgbValues) ;
31 distanceInPixels = sqrt( (xi(2)-xi(1)).^2 + (yi(2)-yi(1)).^2) ;
32 if length(xi) > 2
33 return ;
34 end
35 hold on ;
36 lastDrawnHandle = plot(xi, yi, 'y-', 'LineWidth', 2) ;
37 distanceInUnits = 5.00 ; % cm
38 distancePerPixel = distanceInUnits / distanceInPixels
39
40 % Enter the start of the square area and the length of the area in pixels,
41 % and convert the image to confirm if calibration was successful
42 xstart = 519 ;
43 ystart = 792 ;
44 xlength = 721 ;
45 ylength = 721 ;
46 img = I ;
47 H = img(ystart+(1:ylength), xstart+(1:xlength)) ;
48 xWorldLimits = [0 5] ;
49 yWorldLimits = [-5 0] ;
50 scale = imref2d(size(H), xWorldLimits, yWorldLimits)
51 figure
52 imshow(H, scale) ;
```

Listing E.2: Matlab script for needle end-point data collection

```

1  clc;
2  close all;
3  clear all;
4  workspace;
5
6  % Load all images from this measurement
7  fileFolder = fullfile('H:\Documenten\Studie\Afstuderen\Metingen experiment
8  1\5mms120rpm10Hz\Measurements21');
9  dirOutput = dir(fullfile(fileFolder, '5mms120rpm10Hz'*.jpeg'));
10 fileNames = -dirOutput.name''
11 numFrames = numel(fileNames)
12 %%
13 datasheetName = 'testdata21.xlsx';
14
15 format long g;
16 format compact;
17 fontSize = 20;
18
19 % Here, the specific values for creating the square area of the rulers are
20 % defined
21 xstart = 519;
22 ystart = 792;
23 xlength = 721;
24 ylength = 721;
25
26 % Setting the axes
27 xWorldLimits = [0 5];
28 yWorldLimits = [-5 0];
29
30 %% Collecting the needle end-point manually for each photo and storing it in
31 % a matrix
32 for i = 1:17
33     img = imread(fileNames-i '');
34     grayscale = rgb2gray(img);
35     img = grayscale;
36     H = img(ystart+(1:ylength), xstart+(1:xlength));
37     scale = imref2d(size(H), xWorldLimits, yWorldLimits)
38     figure
39     imshow(H, scale);
40     [xneedle(i), yneedle(i)] = ginput;
41 end
42 %% Converting and saving the needle end-points to a datasheet
43 B = [xneedle', -yneedle'];
44 writematrix(B, datasheetName, 'Sheet', 1, 'Range', 'A1:B17')
45 writematrix(B, 'datatest21.xls')
46
47 %% Loading the coordinates and calculating the standard deviation and
48 % variance
49 filenameSheet = 'H:\Documenten\Studie\Afstuderen\Metingen experiment 1\5
50 mms120rpm10Hz\Measurements21\datatc17.mat'
51 needleCoordinates = load(filenameSheet);
52 needleCoor = needleCoordinates.testdata21;
53 needleCoor = needleCoor-:,:;
54 w = 0;
55 standdev = std(needleCoor, w)
56 variance = var(needleCoor, w)
57 %% Plotting the needle end-point positions and boxplots
58 figure
59 scatter(needleCoor(:,1), needleCoor(:,2))
60 axis([0 5 0 5])
61 xlabel('X-coordinate')
62 ylabel('Y-coordinate')
63 title('Needle positions test condition 17: 5 mm/s and 120 rpm at 10 Hz')
64
65 figure
66 boxplot(needleCoor(:,1))
67
68 figure
69 boxplot(needleCoor(:,2))

```

Listing E.3: Matlab script for plotting the standard deviation

```

1  clc;
2  close all;
3  clear all;
4  workspace;
5
6  X'llaag'cont = [0 0.0331080159731843;30 0.0148833255493562;90
7  0.00654592821012613;120 0.010582358166923128];
8  Y'llaag'cont = [0 0.0185278542845902;30 0.0147258256081495;90
9  0.00888440728889488;120 0.01728830695576128];

```

```

8
9 X'2lagen`cont = [0 0.0252203422914731;30 0.0182150919455248;90
10 0.0199479473860078;120 0.0139519902133214];
11 Y'2lagen`cont = [0 0.0170418841659742;30 0.0112251060545776;90
12 0.00809521161957637;120 0.0129321849213665];
13
14 X'1laag`10Hz = [0 0.0285949761415477;30 0.0153213505204982;60
15 0.0109107613438192;90 0.0111177233188193;120 0.0141347948417302];
16 Y'1laag`10Hz = [0 0.0219751837237351;30 0.0130463393976073;60
17 0.0174512585860191;90 0.00971536591304566;120 0.0112984504774885];
18
19 X'2lagen`10Hz = [0 0.0153271354368909;30 0.0213318791052307;60
20 0.0300516820983161;90 0.0114194946329637;120 0.013424246522145];
21 Y'2lagen`10Hz = [0 0.0160855719283598;30 0.0153882627640632;60
22 0.0230268866665977;90 0.00756465944805544;120 0.0106946256736739];
23
24 figure
25 plot(X'1laag`cont(:,1), X'1laag`cont(:,2), Y'1laag`cont(:,1), Y'1laag`cont(:,2))
26 legend('X', 'Y', 'NorthWest')
27 xlabel('RPM'), ylabel('Standard deviation in mm')
28 title('Standard deviation for continuous actuation in 1 layer of gelatin')
29 ylim([0.004 0.035])
30
31 figure
32 plot(X'2lagen`cont(:,1), X'2lagen`cont(:,2), Y'2lagen`cont(:,1), Y'2lagen`cont
33 (:,2))
34 legend('X', 'Y', 'NorthWest')
35 xlabel('RPM'), ylabel('Standard deviation in mm')
36 title('Standard deviation for continuous actuation in 2 layers of gelatin')
37 ylim([0.004 0.035])
38
39 figure
40 plot(X'1laag`10Hz(:,1), X'1laag`10Hz(:,2), Y'1laag`10Hz(:,1), Y'1laag`10Hz(:,2))
41 legend('X', 'Y', 'NorthWest')
42 xlabel('RPM'), ylabel('Standard deviation in mm')
43 title('Standard deviation for 10 Hz actuation in 1 layer of gelatin')
44 ylim([0.004 0.035])
45
46 figure
47 plot(X'2lagen`10Hz(:,1), X'2lagen`10Hz(:,2), Y'2lagen`10Hz(:,1), Y'2lagen`10Hz
48 (:,2))
49 legend('X', 'Y', 'NorthWest')
50 xlabel('RPM'), ylabel('Standard deviation in mm')
51 title('Standard deviation for 10 Hz actuation in 2 layers of gelatin')
52 ylim([0.004 0.035])
53
54 figure
55 plot(X'1laag`cont(:,1), X'1laag`cont(:,2), X'1laag`10Hz(:,1), X'1laag`10Hz(:,2))
56 legend('Continuous', '10 Hz', 'NorthWest')
57 xlabel('RPM'), ylabel('Standard deviation in mm')
58 title('Standard deviation for X-coordinate in 1 layer of gelatin')
59 ylim([0.004 0.035])
60
61 figure
62 plot(Y'1laag`cont(:,1), Y'1laag`cont(:,2), Y'1laag`10Hz(:,1), Y'1laag`10Hz(:,2))
63 legend('Continuous', '10 Hz', 'NorthWest')
64 xlabel('RPM'), ylabel('Standard deviation in mm')
65 title('Standard deviation for Y-coordinate in 1 layer of gelatin')
66 ylim([0.004 0.035])
67
68 figure
69 plot(X'2lagen`cont(:,1), X'2lagen`cont(:,2), X'2lagen`10Hz(:,1), X'2lagen`10Hz
70 (:,2))
71 legend('Continuous', '10 Hz', 'NorthWest')
72 xlabel('RPM'), ylabel('Standard deviation in mm')
73 title('Standard deviation for X-coordinate in 2 layers of gelatin')
74 ylim([0.004 0.035])

```

Listing E.4: Matlab script for two-sample F-test

```

1  clc;
2  close all;
3  clear all;
4
5  %% For continuous actuation in one layer of gelatin
6  % No rotation
7  file0 = 'H:\Documenten\Studie\Afstuderen\Metingen experiment 1\5mms0rpm\
      Measurements2\datatc2.mat';
8  needleCoordinates0 = load(file0);
9  needleCoor0 = needleCoordinates0.testdata2;
10 needleCoor0 = needleCoor0-:,:";
11 data`0x = needleCoor0(:,1);
12 data`0y = needleCoor0(:,2);
13
14 % 120 rpm
15 file120 = 'H:\Documenten\Studie\Afstuderen\Metingen experiment 1\5mms120rpm\
      Measurements1\datatc1.mat';
16 needleCoordinates120 = load(file120);
17 needleCoor120 = needleCoordinates120.datatest1;
18 needleCoor120 = needleCoor120-:,:";
19 data`120x = needleCoor120(:,1);
20 data`120y = needleCoor120(:,2);
21
22 % 90 rpm
23 file90 = 'H:\Documenten\Studie\Afstuderen\Metingen experiment 1\5mms90rpm\
      Measurements8\datatc5.mat';
24 needleCoordinates90 = load(file90);
25 needleCoor90 = needleCoordinates90.testdata8;
26 needleCoor90 = needleCoor90-:,:";
27 data`90x = needleCoor90(:,1);
28 data`90y = needleCoor90(:,2);
29
30 % 30 rpm
31 file30 = 'H:\Documenten\Studie\Afstuderen\Metingen experiment 1\5mms30rpm\
      Measurements7\datatc4.mat';
32 needleCoordinates30 = load(file30);
33 needleCoor30 = needleCoordinates30.testdata7;
34 needleCoor30 = needleCoor30-:,:";
35 data`30x = needleCoor30(:,1);
36 data`30y = needleCoor30(:,2);
37
38 % Performing the two-sample F-test:
39 [h1x,p1x] = vartest2(data`0x,data`120x)
40 [h1y,p1y] = vartest2(data`0y,data`120y)
41 [h2x,p2y] = vartest2(data`0x,data`90x)
42 [h2y,p2y] = vartest2(data`0y,data`90y)
43 [h3x,p3x] = vartest2(data`0x,data`30x)
44 [h3y,p3y] = vartest2(data`0y,data`30y)

```

F

STANDARD DEVIATION

The standard deviation is organized per coordinate, number of layers and actuation frequency. The values are given as calculated in Matlab. However, the significance should be three digits, as the values are obtained using the length scale of 5.00 cm.

Coord, layer, freq	0	30	60	90	120
x, 1, cont	0.0331080159731843	0.01488333255493562	-	0.000654592821012613	0.010582358166923128
y, 1, cont	0.0185278542845902	0.0147258256081495	-	0.000888440728889488	0.01728830695576128
x, 2, cont	0.02522034222914731	0.0182150919455248	-	0.0199479473860078	0.0139519902133214
y, 2, cont	0.0170418841659742	0.0112251060545776	-	0.00809521161957637	0.0129321849213665
x, 1, 10 Hz	0.0285949761415477	0.0153213505204982	0.0109107613438192	0.0111177233188193	0.0141347948417302
y, 1, 10 Hz	0.0219751837237351	0.0130463393976073	0.0174512585860191	0.00971536591304566	0.0112984504774885
x, 2, 10 Hz	0.0153271354368909	0.0213318791052307	0.0300516820983161	0.0114194946329637	0.013424246522145
y, 2, 10 Hz	0.0160855719283598	0.0153882627640632	0.023026886665977	0.00756465944805544	0.0106946256736739
x, 1, 5 Hz	-	-	-	-	0.0109013042177665
y, 1, 5 Hz	-	-	-	-	0.00920895714060843

Figure F.1: Standard deviation

